Draft version December 15, 2017
Typeset using LaTeX **twocolumn** style in AASTeX61

NO TIME FOR DEAD TIME - USE THE FOURIER AMPLITUDE DIFFERENCES TO NORMALIZE DEAD TIME-AFFECTED PERIODOGRAMS

Matteo Bachetti[1] and Daniela Huppenkothen[2,3]

[1] *INAF-Osservatorio Astronomico di Cagliari, via della Scienza 5, I-09047 Selargius (CA)*
[2] *Center for Data Science, New York University, 60 5h Avenue, 7th Floor, New York, NY 10003*
[3] *Center for Cosmology and Particle Physics, Department of Physics, New York University, 4 Washington Place, New York, NY 10003, USA*

(Received XXXX; Revised XXXX; Accepted December 15, 2017)

Submitted to ApJL

ABSTRACT

Dead time affects many of the instruments used in X-ray astronomy, by producing a strong distortion in power density spectra. This can make it difficult to model the aperiodic variability of the source or look for quasi-periodic oscillations. Whereas in some instruments a simple a-priori correction for dead time-affected power spectra is possible, this is not the case for others such as *NuSTAR*, where the dead time is non-constant and long ($\sim$2.5 ms). Bachetti et al. (2015) suggested the cospectrum obtained from light curves of independent detectors within the same instrument as a possible way out, but this solution has always only been a partial one: the measured r.m.s. was still affected by dead time, because the width of the power distribution of the cospectrum was modulated by dead time in a frequency-dependent way.

In this Letter we suggest a new, powerful method to normalize deadtime-affected cospectra and power density spectra. Our approach uses the difference of the Fourier amplitudes from two independent detectors to characterize and filter out the effect of dead time. This method is crucially important for the accurate modeling of periodograms derived from instruments affected by dead time on board current missions like *NuSTAR* and *Astrosat*, but also future missions such as *IXPE*.

Keywords: X-rays: binaries — X-rays: general — methods: data analysis — methods: statistical

Corresponding author: Matteo Bachetti
bachetti@oa-cagliari.inaf.it

1. INTRODUCTION

Dead time is an unavoidable and common issue of photon-counting instruments. It is the time t_d that the instrument takes to process an event and be ready for the next event. In most current astronomical photon-counting X-ray missions, dead time is of the *non-paralyzable* kind, meaning that the instrument does not accept new events during dead time, avoiding a complete lock of the instrument if the incident rate of photons is higher than $1/t_d$. Being roughly energy-independent, dead time is not usually an issue for spectroscopy, as it only affects the maximum rate of photons that can be recorded, so it basically only increases the observing time needed for high quality spectra.

For timing analysis, the effect of dead time is far more problematic. The periodogram, commonly referred to as power density spectrum (PDS)[1], which is the most widely used statistical tool to investigate rapid variability, is heavily distorted by dead time, with a characteristic pattern similar to a damped oscillator. This pattern is stronger for brighter sources, and it is often not possible to disentangle this power spectral distortion due to dead time and the broadband noise components characterizing the emission of accreting systems. In the special case where dead time is constant, its shape can be modeled precisely (Zhang et al. 1995; Vikhlinin et al. 1994). However, dead time is often different on an event-to-event basis (e.g., in *NuSTAR*), and it is not obvious how to model it precisely, also because the information on dead time is often incomplete in the data files distributed by HEASARC (see, e.g. Bachetti et al. 2015).

When using data from missions carrying two or more *identical and independent* detectors like *NuSTAR*, Bachetti et al. (2015) proposed an approach to mitigate instrumental effects like dead time exploiting this redundancy: where in standard analysis, light curves of multiple detectors are summed before Fourier transforming the summed light curve, it is possible to instead Fourier-transform the signal of two independent detectors and combine the Fourier amplitudes in a *cospectrum* – the real part of the cross spectrum – instead of the periodogram. Since dead time is uncorrelated between the two detectors, the resulting powers have a mean white noise level fixed to 0, which resolves the first and most problematic issue created by dead time (see details in Bachetti et al. 2015); however, the resulting powers no longer follow the statistical distribution expected for power spectra, and their probability distribution is frequency-dependent. Whereas a noise cospectrum in the absence of dead time would follow a Laplace distribution (Huppenkothen and Bachetti, sub.), dead time affects the width of the probability distribution for cospectral powers and modulates the measured r.m.s. similarly to the distortion acted on power spectra. In this Letter, we show a method to precisely recover the shape of the power density spectrum by looking at the difference of the Fourier amplitudes of the light curves of two independent detectors. This difference, in fact, contains information on the uncorrelated noise produced by dead time, but not on the source-related signal which is correlated between the two detectors. This allows to disentangle the effects of dead time from those of the source variability.

In Section 2 we show that, in the absence of dead time, the difference of the Fourier amplitudes calculated two independent detectors contain the sum of the correlated signal (the source signal) and uncorrelated noise (detector-related noise), and that their difference eliminates the source part. In Section 3 we use extensive simulations to show how to use this fact to correct deadtime-affected periodograms, and we describe the limitations of this method.

2. ON THE DIFFERENCE OF FOURIER AMPLITUDES

Let us consider two identical and independent detectors observing the same variable source, producing independent and strictly simultaneous time series, with identical even sampling δt, $\mathbf{x} = \{x_k\}_{k=1}^{N}$ and $\mathbf{y} = \{y_k\}_{k=1}^{N}$. For a stochastic process (e.g. $1/\nu$-type red noise), the Fourier amplitudes will vary as a function of $N_{\rm phot}P(\nu)/4$, where $P(\nu)$ (Leahy-normalized, Leahy et al. 1983) is the shape of the power spectrum underlying the stochastic process, and $N_{\rm phot}$ denotes the number of photons in a light curve.

If the two detectors observe the same source simultaneously, the amplitudes and phases of the stochastic process will be shared among $\mathbf{x}$ and $\mathbf{y}$, while each light curve will be affected *independently* by the photon counting noise in the detector, as well as the dead time process.

Dead time can be considered a convolution on the signal (Vikhlinin et al. 1994). Following the convolution theorem the Fourier transform $\mathcal{F}$ of dead time-affected light curves will be the *product* of the Fourier transform of the signal $\mathcal{S}$ and the Fourier transform of the dead time filter $\mathcal{D}$:

$$\mathcal{F}(\nu) = \mathcal{S}(\nu) \cdot \mathcal{D}(\nu) \tag{1}$$

[1] here we will use the term PDS for the actual source power spectrum, and *periodogram* to indicate our estimate of it, or otherwise said, the realization of the "real" power spectrum we observe in the data

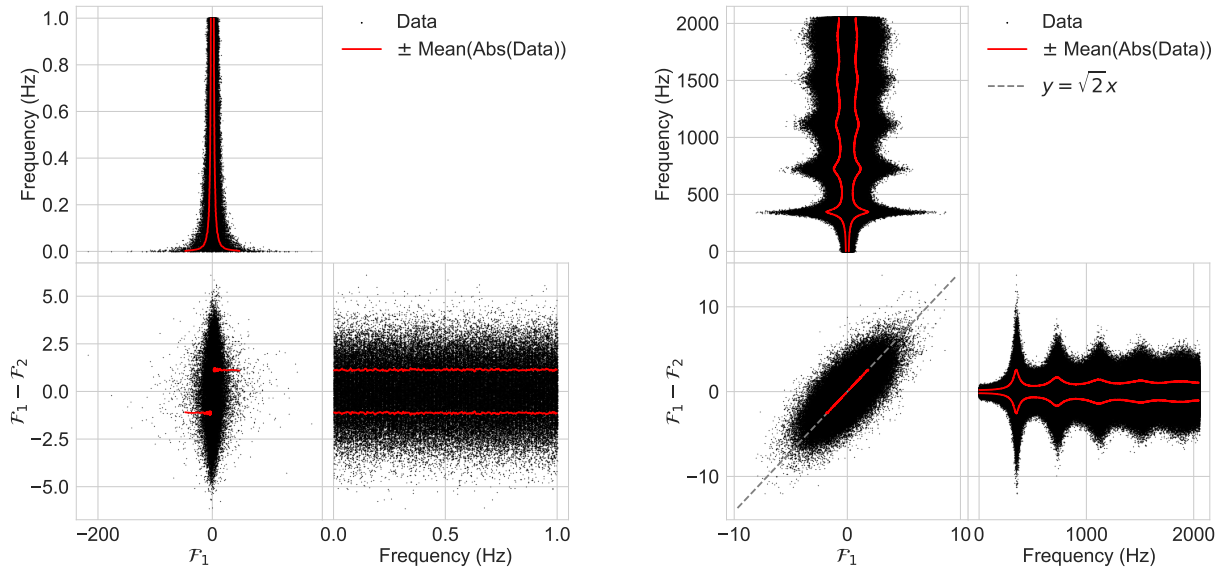

Figure 1. Real-valued Fourier amplitudes obtained by single light curves ($\mathcal{F}_1$) and difference between two realizations of the same source light curve ($\mathcal{F}_1 - \mathcal{F}_2$), plotted against each other in two cases: (Left) Strong $1/f$ red noise and no dead time, calculated over many 500 s segments of the light curve, and (Right) no red noise and strong dead time, calculated over 5 s segments of the light curve. The red curve gives the frequency-dependent spread of the distributions, measured by the mean of the absolute values of the curves in each frequency bin. The different behavior of Fourier amplitude differences in the two cases is evident: in the deadtime-free case, the Fourier amplitude difference does *not* correlate with the Fourier amplitude, while in the deadtime-affected case, this follows a precise linear relationship.

For a large enough number of data points N, the complex Fourier amplitudes S_j will be composed of a sum of two independent random normal variables for the intrinsic red noise variability and the detector photon counting noise, respectively: $S_j = S_{sj} + S_{nj}$, with $\Re(S_{sj}) \sim \mathcal{N}(0, \sigma_{sj}^2)$ and $\Re(S_{nj}) \sim \mathcal{N}(0, \sigma_n^2)$, and similarly for the imaginary parts. The red noise variance $\sigma_{sj}^2 = \sigma_s^2(\nu) = N_{\rm phot} P(\nu)/4$ (where $N_{\rm phot} = \sum_{k=1}^{N} x_k$) is given by the power spectrum of the underlying stochastic process and is frequency-dependent. However, the photon counting noise $\sigma_n^2 = N_{\rm phot}/2$ is independent of frequency. Note that $S_{xsj} = S_{ysj}$, because the amplitudes of the stationary noise process will be the same for the Fourier transforms of $\mathbf{x}$ and $\mathbf{y}$ for the case considered here, while the components due to white noise differ between the two time series. The dead time filter affects the sum of signal and white noise amplitudes as a multiplicative factor and only depends on count rate, which is equal for both light curves given identical detectors. Thus, the difference between the Fourier amplitudes for the two time series $\mathbf{x}$ and $\mathbf{y}$ will be:

$$F_{xj} - F_{yj} = (S_{xj} - S_{yj}) \cdot D_j = (S_{xnj} - S_{ynj}) \cdot D_j \quad (2)$$

Because $S_{xsj} = S_{ysj}$, but $S_{xnj} \neq S_{ynj}$ (since the white noise component is formed in each detector separately), the *difference* of the real and imaginary Fourier amplitudes between the two light curves effectively encodes the white noise component only, multiplied by the Fourier transform of the dead time filter. This fact effectively allows us to separate out the (source-intrinsic) red noise from the spurious variability introduced by dead time: if we can extract the shape of the dead time filter $|\mathcal{D}|^2$ from the Fourier amplitude differences of the two detectors, we can use it to correct the shape of the periodogram. In the following section, we lay this procedure out in more detail, and describe its limits in Section 3.5.

3. THE FAD METHOD

3.1. *Data simulation*

All simulated and real data sets in this paper were produced and/or analyzed with a combination of the two Python libraries `stingray`[2] (Huppenkothen et al. 2016) and `HENDRICS` v.`3.0b2` (formerly known as MaLTPyNT; Bachetti 2015), both based on Astropy (Astropy Collaboration et al. 2013).

We used the same procedure and algorithms described by Bachetti et al. (2015), Section 4, which we briefly summarize here. We used the Timmer & Koenig (1995) method to create a red noise light curve starting from a given power spectral shape. This method is im-

[2] The library is under heavy development. For this work we used the version identified by the hash `3e64f3d`. See https://github.com/StingraySoftware/notebooks/ for tutorials on simulations, light curve production and timing analysis with Stingray

plemented in the `stingray.simulate` module. This step needs to be done carefully: if the initial light curves contain significant random noise, the process for the creation of events creates a random variate on the top of the local count rate–which is varying randomly already–producing a non-Poissonian final light curve. We initially simulated light curves with a very high mean "count rate" such that the Poisson noise was relatively small. We then renormalized the light curves to the wanted (lower) count rate and r.m.s. and finally used these light curves to simulate event lists using rejection sampling, implemented in the `stingray.Eventlist.simulate_times()` method. Then, the `hendrics.fake.filter_for_deadtime()` function was used to apply a non-paralyzable dead time of 2.5 ms to the simulated event lists. For more details on the simulated data sets, see also Section 3.4 and the available Jupyter notebooks[3] (for a description of Jupyter notebooks, see Kluyver et al. 2016). After producing these synthetic event lists, we started the standard timing analysis: we produced light curves with a bin time of ~ 0.122 ms, and calculated power spectral products (cospectrum, periodogram) over segments of these light curves using `stingray`.

3.2. *First test: white noise*

As laid out in Section 2, the difference of Fourier amplitudes from two independent but identical detectors shows no source variability, but *still shows the same distortion* due to dead time (See Figure 1, left panel, where this is shown with red noise). Let us simulate two constant light curves with an incident mean count rate of 400 counts/sec and a dead time of 2.5 ms, as we would expect from the two identical detectors of *NuSTAR* observing the same stable X-ray source. The Fourier amplitudes of the light curves from the two detectors are heavily distorted by dead time, with the characteristic damped oscillator-like shape (Vikhlinin et al. 1994; Zhang et al. 1995) (Figure 1, middle panel). Therefore, using the difference between the Fourier amplitudes in two detectors, we can in principle renormalize the periodogram so that only the source variability alters its otherwise flat shape.

As shown in Figure 1 (right panel), the single-detector Fourier amplitudes are proportional on average to the difference of the Fourier amplitudes in different realizations, with a constant factor $1/\sqrt{2}$. Therefore, we expect that the periodogram will be proportional to the square of the Fourier amplitude difference, divided by 2. Let us try to *divide the periodogram by a smoothed version of the squared Fourier differences*, and multiply by 2. For smoothing, we used a Gaussian running window with a window width of 50 bins. Given that the initial binning had 50 bins/Hz, this interpolation allows an aggressive smoothing over bins whose y value does not change significantly. We call this procedure the **Fourier Amplitude Difference** (hereafter FAD) **correction**.

The results of this correction are shown in Figure 2. Starting from a heavily distorted distribution of the powers, applying the FAD correction "flattens" remarkably well the white noise level of the periodogram and the distribution of the scatter of the white noise periodogram and cospectrum. Also, it reinstates a correct distribution of powers, following the expected χ^2_2 distribution (Lewin et al. 1988) very closely. Analogously, the corrected cospectrum will follow the expected Laplace distribution (Huppenkothen & Bachetti, sub.). While the original dead time-affected cospectrum had a frequency-dependent modification to the r.m.s. level, the FAD-corrected cospectrum gets back to a frequency-independent shape, like in the dead time-free case.

3.3. *The FAD algorithm in detail*

In practice, the FAD correction algorithm in a generic case would work as follows:

1. split the light curves from two independent, identical detectors into segments as one would do to calculate standard averaged periodograms;
2. for each pair of light curve segments:
   - calculate the Fourier transform of each detector separately, and then of the summed detectors (hereafter total-intensity);
   - save the unnormalized Fourier amplitudes;
   - multiply these Fourier amplitudes by $\sqrt{2/N_{ph}}$ (that would give Leahy-normalized periodograms if squared);
   - subtract the Leahy-normalized Fourier amplitudes of the two detectors between them, *take the absolute value*, and obtain this way the Fourier Amplitude Differences (FAD);
   - *smooth* the FAD using a Gaussian-window interpolation with a large number of bins, in our case all the bins contained in 1-2 Hz;
   - use the separated single-detector and total-intensity *unnormalized* Fourier amplitudes to calculate the periodograms (and/or the cospectrum);

[3] https://github.com/matteobachetti/deadtime-paper-II

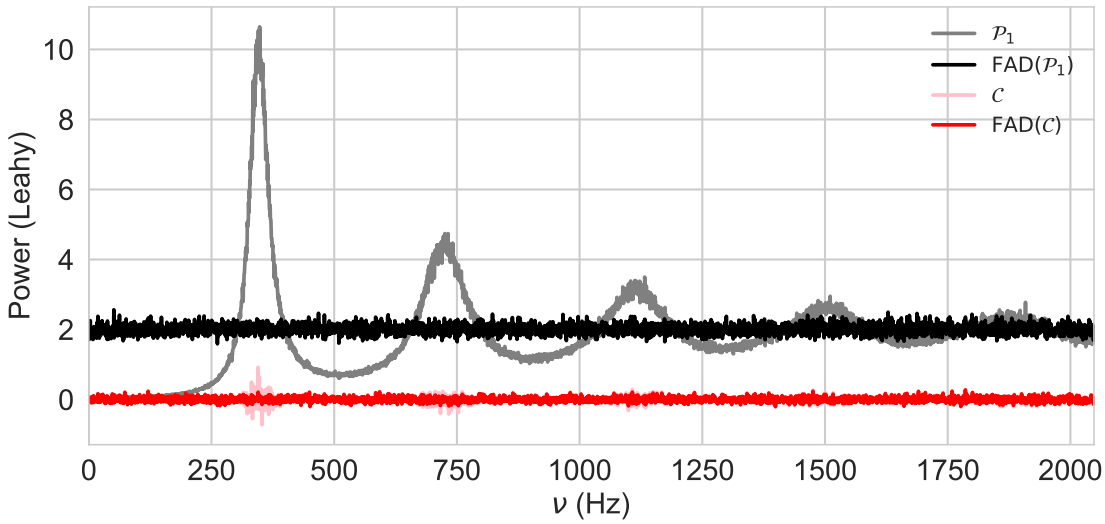

Figure 2. Periodogram and cospectrum, before and after FAD correction, for a pure white noise light curve. The deadtime-driven distortion of the white noise level in the periodogram, and the frequency-dependent modulation of the r.m.s. in both spectra, disappear after applying the FAD correction. Spectra were calculated over 2-sec intervals and averaged, to decrease the scatter and highlight the distortion of powers.

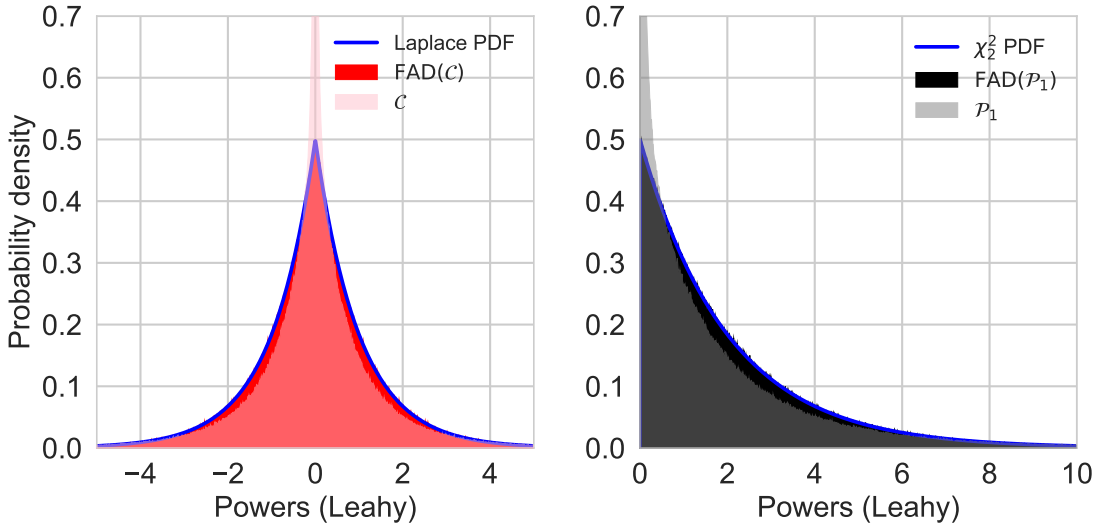

Figure 3. Probability density function of non-averaged powers in the cospectrum (pink) and the periodogram (grey), before the FAD correction and after (red and black, respectively), shown as a fine-grained histogram. After correction, the powers follow remarkably well the expected Laplace (cospectrum) and χ^2_2 (periodogram) distributions, as highlighted by the overplotted probability density functions (PDF).

- divide all periodograms (and/or the cospectrum) by the smoothed and squared FAD, and multiply by 2.

3. normalize the periodograms to the wanted normalization (e.g. Leahy et al. 1983 or fractional r.m.s.: Belloni & Hasinger 1990; Miyamoto et al. 1991).

3.4. *FAD correction of generic variable periodograms*

We are now ready to verify the last step: is the FAD-corrected periodogram equivalent (albeit with some loss of sensitivity due to the lower number of photons) to the dead time-free periodogram? To test this, we produced a number of different synthetic datasets as explained in Section 3.2, containing different combinations of QPOs

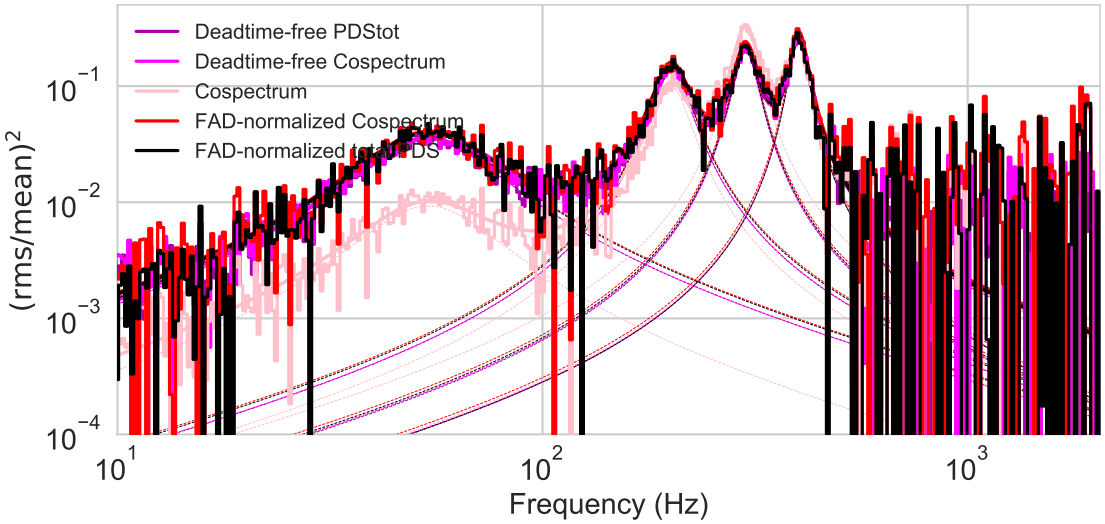

Figure 4. Periodograms and cospectra from a simulation with four Lorentzian features (at 50, 200, 300 and 400 Hz) with 40-Hz full with at half maximum (FWHM). We plotted and fitted periodograms and cospectra before and after applying a 2.5 ms dead time filter The total r.m.s. before dead time was 40% and the incident photon flux 400 ct/s. There is no significant difference between FAD-normalized and deadtime-free periodograms and cospectra, that are almost indistinguishable (note also the agreement between all best-fit Lorentzians). For comparison, we also plot the cospectrum without FAD (pink), showing very different amplitudes for the four Lorentzians, due to dead time.

and broadband noise components.[4] We first calculated the periodogram and cospectrum of the dead time-free data, averaged over 128-s intervals. Then, we applied a dead time filter to the event list and applied the FAD correction, as described in Section 3.3

All spectra were then expressed in fractional r.m.s. normalization, where the integral of the fitted power spectral components over the frequency returns directly its fractional r.m.s.. In the r.m.s. normalization, the values of each point of the periodogram, after white noise subtraction, should be consistent between the dead time-free and the FAD-corrected periodograms. We fitted all spectra with the model which produced the simulated data and checked if the r.m.s. values were consistent with the fit on the dead time-free periodogram. To calculate this r.m.s., we fitted the spectra with two Lorentzian components, and integrated the model over the full frequency range. For periodograms, the model included also a constant offset to account for the white noise level. An example of this analysis is shown in Figure 4: the FAD successfully corrects so well periodograms and cospectra when compared to dead-time free simulated spectra, that in the figure they are almost indistinguishable.

[4] A number of jupyter notebooks is available in the GitHub repo: https://github.com/matteobachetti/deadtime-paper-II to reproduce the full analysis plotted in the Figures of this paper and more. The full algorithm described in Section 3.3 is contained in the `fad_correction.py` file in the notebooks directory, for reference.

3.5. *Simulation results and discussion*

In order to test the robustness of the FAD, we have ran extensive simulations testing how the method performs (1) for a range of different input count rates, leading to dead-time effects of different magnitude in the output periodograms and cospectra, and (2) whenthe light curves do not have the same count rate (since detectors may in reality have slightly different efficiencies). The simulations show that the shape of the periodogram is precisely corrected by the FAD procedure if (1) *the input light curves have the same count rate* and (2) *for values of the input count rate and* r.m.s. *that are not too extreme*. Differing input count rates in different detectors matter in practice only for the single-detector periodogram, but *not* for cospectra and total-intensity periodograms. At high count rates, single-detector periodograms are corrected very well only if the two detectors have very similar count rates, and count rates must be more similar athigher count rates in order for the correction to apply. However, we find that the total-intensity periodogram and the cospectrum remain well corrected by the FAD even if the count rate in the two detectors differs by 30% in most cases. Therefore, we recommend to use the FAD very carefully with single-detector periodograms, which should not be an issue given that the total-intensity periodogram is more sen-

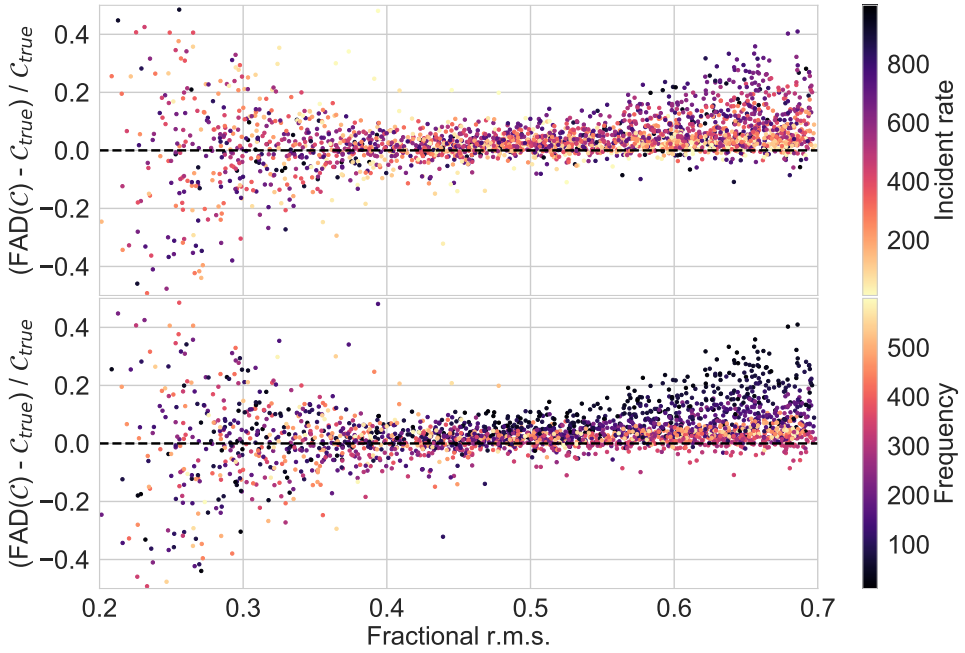

Figure 5. Relative overestimation of FAD with respect to r.m.s., versus r.m.s., as calculated from the cospectrum. We encoded in the color the the incident rate (Top) and the frequency of the feature. From this visualization we see two regimes: below ∼40% fractional r.m.s., the errors are dominated by statistical errors. These errors will simply decrease when we average more data, as we expect from statistical errors. Over ∼40% fractional r.m.s., the errors are significantly skewed towards an overestimation of the r.m.s., and this is clearly truer when the incident rate *and* the r.m.s. are high, and the frequency relatively low (as can be seen by the fact that the distribution of darker points in both plots is more skewed towards positive values).

sitive and more convenient to use. A comparison with the cospectrum, which is not affected by white noise level distortions, is always recommended.

However, we find that the FAD correction consistently overestimates the integrated r.m.s. when the count rate and r.m.s. are *both* very high, *in particular at low frequency* (See Figure 5). At ∼200 ct/s and 50% r.m.s., the relative overestimation is below 5% (meaning that if the true r.m.s. is 50%, the measured r.m.s. is between 50 and 53%) and it is symmetrically distributed around 0, as expected from statistical uncertainties. At higher incident rates and r.m.s., the uncertainty distribution is biased towards positive relative errors, implying an overestimation of the r.m.s.. This should not be a problem in most use cases, when the r.m.s. is used as a rough indicator for spectral state. If very precise measurements of r.m.s. are needed (for example, to calculate r.m.s./energy spectra), it is safer to account for this bias through simulations. As a rough rule-of-thumb, the bias in the measured fractional r.m.s. increases *linearly* with the count rate and *quadratically* with r.m.s.. A practical way to estimate this effect during analysis is to apply the FAD, obtain a best fit model, calculate the r.m.s., and simulate a number of realizations of the light curve to evaluate the amount of overestimation involved[5].

4. CONCLUSIONS

In this Letter we described a method to correct the normalization of dead time-affected periodograms. This method is valid in principle for 1) correcting the shape of the periodogram, eliminating the well known pattern produced by dead time, and 2) adjusting the white noise standard deviation of periodogram and cospectra to its correct value at all frequencies. In general, we recommend applying the FAD correction to both the periodogram and the cospectrum. The periodogram, if obtained by the sum of the light curves, can yield a higher signal-to-noise ratio. However, the white noise level subtraction is not always very precise due to mismatches in the mean count rate in the two light curves. A comparison with the FAD-corrected cospectrum, to verify visually the white noise subtraction, is always recom-

[5] relevant code can be found in Jupyter notebooks in the following GitHub repository: https://github.com/matteobachetti/deadtime-paper-II

mended: the white noise subtraction is the most important step when calculating the significance of a given feature in the periodogram (e.g. Barret & Vaughan 2012; Huppenkothen et al. 2017). The cospectrum has indeed the advantage of not requiring white noise level subtraction.

We performed a number of simulations to test the validity of our method and explore its performance in the limits of high count rates as well as detectors with mis-matched efficiencies. In all cases, we find that the adjustment of the white noise standard deviation in the periodogram and the cospectrum works remarkably well, allowing to make a confident analysis of X-ray variability even in sources where this was precluded until now. Only in cases where the count rate and the r.m.s. are *both* very high (>500 ct/s incident, >40% resp.), the FAD correction leads to an overestimation the r.m.s., even if the white noise level of the periodogram remains flat.

We thank the anonymous referee for providing very helpful feedback. We thank David W. Hogg for useful discussions on the topic of Fourier analysis, and Jeff Scargle for useful suggestions and comments. MB is supported in part by the Italian Space Agency through agreement ASI-INAF n.2017-12-H.0 and ASI-INFN agreement n.2017-13-H.0. DH is supported by the James Arthur Postdoctoral Fellowship and the Moore-Sloan Data Science Environment at New York University.

REFERENCES

Astropy Collaboration, Robitaille, T. P., Tollerud, E. J., et al. 2013, A&A, 558, A33

Bachetti, M. 2015, Astrophysics Source Code Library, ascl:1502.021

Bachetti, M., Harrison, F. A., Cook, R., et al. 2015, ApJ, 800, 109

Barret, D., & Vaughan, S. 2012, ApJ, 746, 131

Belloni, T., & Hasinger, G. 1990, A&A, 230, 103

Huppenkothen, D., Bachetti, M., Stevens, A. L., Migliari, S., & Balm, P. 2016, Stingray: Spectral-timing software, Astrophysics Source Code Library, , , ascl:1608.001

Huppenkothen, D., Younes, G., Ingram, A., et al. 2017, ApJ, 834, 90

Kluyver, T., Ragan-Kelley, B., Pérez, F., et al. 2016, in ELPUB, 87–90

Leahy, D. A., Darbro, W., Elsner, R. F., et al. 1983, ApJ, 266, 160

Lewin, W. H. G., van Paradijs, J., & van der Klis, M. 1988, SSRv, 46, 273

Miyamoto, S., Kimura, K., Kitamoto, S., Dotani, T., & Ebisawa, K. 1991, ApJ, 383, 784

Timmer, J., & Koenig, M. 1995, A&A, 300, 707

Vikhlinin, A., Churazov, E., & Gilfanov, M. 1994, 287, 73

Zhang, W., Jahoda, K., Swank, J. H., Morgan, E. H., & Giles, A. B. 1995, ApJ, 449, 930